Dalton Transactions

PAPER

View Article Online
View Journal | View Issue

Cite this: *Dalton Trans.*, 2017, **46**, 3547

Radical anion and dianion salts of titanyl macrocycles with acceptor substituents or an extended π-system†

Maxim A. Faraonov,[a] Dmitri V. Konarev,*[a] Alexey M. Fatalov,[a,b] Salavat S. Khasanov,[c] Sergey I. Troyanov[b] and Rimma N. Lyubovskaya[a]

Received 28th December 2016,
Accepted 16th February 2017

DOI: 10.1039/c6dt04896j

rsc.li/dalton

Crystalline anionic salts of titanyl macrocycles with acceptor substituents or an extended π-system have been obtained for the first time: $(PPN^+)_2\{O{=}Ti^{IV}(PcCl_8^{4-})\}^{2-}$ (**1**), $(PPN^+)\{O{=}Ti^{IV}(Nc^{\bullet 3-})\}^{\bullet -}\cdot 2C_6H_4Cl_2$ (**2**) and $(PPN^+)_2\{O{=}Ti^{IV}(AceTPrzPz^{4-})\}^{2-}\cdot 1.3C_6H_4Cl_2\cdot 0.8C_6H_5CN$ (**3**) where PPN^+ is the bis(triphenylphosphoranylidene)ammonium cation, $PcCl_8$ – 2,3,9,10,16,17,23,24-octachlorophthalocyanine; Nc – 2,3-naphthalocyanine, AceTPrzPz – tetra(acenaphthenopyrazino)porphyrazine. Salts **1–3** were obtained in the reduction of the parent titanyl macrocycles by fluorenone ketyl in the presence of an excess of PPNCl in *o*-dichlorobenzene with following precipitation of crystals with *n*-hexane. Reduction of macrocycles in **1–3** is accompanied by the appearance of intense NIR bands in the solid spectra at 963–1159 nm. It has been found that the extended π-system with linear annulation in $\{O{=}Ti^{IV}(Nc^{\bullet 3-})\}^{\bullet -}$ provides the shift of the NIR band to smaller energies (1159 nm) in comparison with those in the spectra of $\{O{=}Ti^{IV}(Pc^{\bullet 3-})\}^{\bullet -}$ (995–998 nm). Reduction of macrocycles leads also to the alternation of C–N_{imine} bonds due to partial disruption of their aromaticity. The disruption is higher for the dianions in **1** and **3** in comparison with the radical anions in **2**. One-dimensional π–π stacking chains and layers are formed in **1** and **3** with diamagnetic $\{O{=}Ti^{IV}(PcCl_8^{4-})\}^{2-}$ and $\{O{=}Ti^{IV}(AceTPrzPz^{4-})\}^{2-}$ dianions, respectively. Salt **2** contains nearly isolated $[\{O{=}Ti^{IV}(Nc^{\bullet 3-})\}^{\bullet -}]_2$ dimers with a strong π–π interaction between paramagnetic radical anion macrocycles. As a result, a transition from the triplet to singlet state with antiparallel ordering of spins within the dimers is observed in **2** below 200 K.

Introduction

Metal phthalocyanine compounds possess promising optical, conducting and magnetic properties. Some phthalocyanine derivatives can be used as sensors and materials for optical, electronic and photoelectronic devices.[1,2] Conducting compounds can be obtained by oxidation of phthalocyanines or axially substituted phthalocyanine anions $\{M^{III}L_2(Pc^{2-})\}^-$ (M = Co, Fe; L = CN, Cl, Br) to produce crystalline salts with quasi-one-dimensional metallic behavior down to liquid helium temperatures. These salts have π–π stacking columnar arrangement of the macrocycles.[3,4] Since some metal phthalocyanines contain paramagnetic metals they are also used as active components in the design of magnetic compounds. For example, oxidation of substituted manganese(II) naphthalocyanine with tetracyanoethylene or reduction of iron(II) phthalocyanine with decamethylchromocene yields compounds with the alternation of ions and ferrimagnetic ordering of spins.[5,6]

Several radical anion and dianion salts of metal phthalocyanines were also synthesized as single crystals.[7–21] Crystalline anionic salts were obtained in the reduction of Mg^{II}, $O{=}Nb^{IV}$, Al^{III}, Ge^{IV} and Zr^{IV} phthalocyanines with Na/Hg, potassium graphite (KC_8) or LiCp*.[7–11] Salts with reduced cobalt(II) and iron(II) phthalocyanines,[12–16] iron(II) hexadecachlorophthalocyanine,[17,18] and a large series of radical anion $\{M(Pc^{\bullet 3-})\}^{\bullet -}$ salts, M = Cu^{II}, Ni^{II}, H_2, Sn^{II}, Pb^{II}, $O{=}Ti^{IV}$, $O{=}V^{IV}$, $Sn^{IV}Cl_2$ and $In^{III}Br$, were also obtained and structurally characterized.[19–22] Nevertheless, until now no anionic salts of such a type were obtained with other macrocycles except for phthalocyanines. These macrocycles can contain acceptor substituents to stabilize their radical anions in air or an extended π-system allowing the synthesis of structures with stronger π–π interactions. Reduction of metal macrocycles can also be used to obtain

[a]*Institute of Problems of Chemical Physics RAS, Chernogolovka, Moscow region, 142432, Russia. E-mail: konarev3@yandex.ru*
[b]*Moscow State University, Leninskie Gory, 119991 Moscow, Russia*
[c]*Institute of Solid State Physics RAS, Chernogolovka, Moscow region, 142432, Russia*

†Electronic supplementary information (ESI) available: The IR spectra of the starting compounds and salts **1–3**. CCDC 1518488, 1518412 and 1518411. For ESI and crystallographic data in CIF or other electronic format see DOI: 10.1039/c6dt04896j

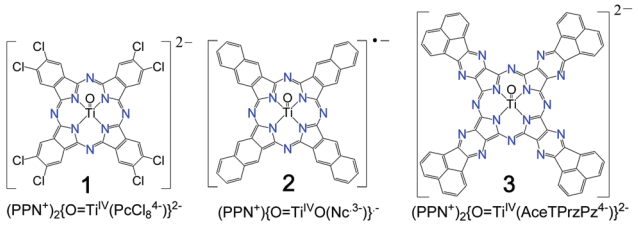

Scheme 1

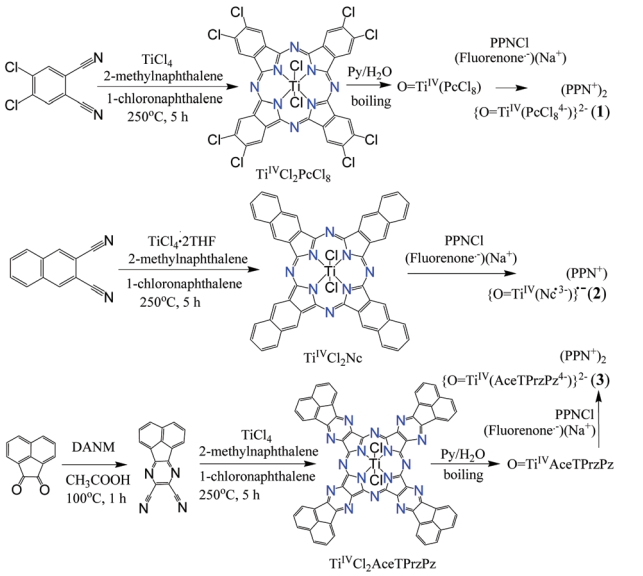

Scheme 2

them in a crystalline form since in spite of the large size of the macrocycles they are well soluble in organic solvents in radical anion and dianion states.

Titanyl phthalocyanine is a well-known organic photoconductor which shows very good photoconductivity, excellent photostability, and wide absorption in the visible region with high absorbance.[2,23–25] Until now several substituted titanyl and vanadyl phthalocyanines were obtained.[26–28] However, the molecular structure was determined for unsubstituted titanyl and vanadyl phthalocyanines only using the Rietveld method on powdered samples[29,30] or crystals,[31] respectively.

In this work we chose titanyl macrocycles to introduce acceptor substituents or an extended π-system. We dissolve them in *o*-dichlorobenzene by their reduction and crystallize radical anion and dianion salts of titanyl octachlorophthalocyanine in $(PPN^+)_2\{O{=}Ti^{IV}(PcCl_8^{4-})\}^{2-}$ (**1**), titanyl naphthalocyanine in $(PPN^+)\{O{=}Ti^{IV}(Nc^{\bullet 3-})\}^{\bullet -}\cdot 2C_6H_4Cl_2$ (**2**) and tetra(acenaphthenopyrazino)porphyrazine in $(PPN^+)_2\{O{=}Ti^{IV}(AceTPrzPz^{4-})\}^{2-}\cdot 1.3C_6H_4Cl_2\cdot 0.8C_6H_5CN$ (**3**) (Scheme 1). Preparation of single crystals of these salts allows us to determine the molecular structures of titanyl macrocycles including that of AceTPrzPz (Scheme 1) which is one of the largest macrocycles among tetrapyrazinoporphyrazines.[32] We provide information on the reduction effect on the molecular structures, optical and magnetic properties of titanyl macrocycles.

Results and discussion

Synthesis

Titanium dichloride macrocycles were synthesized by tetramerization of the corresponding dicarbonitriles in the presence of $TiCl_4$ or $TiCl_4\cdot 2THF$ in 1-chloronaphthalene in 68–75% yield. Addition of 2-methylnaphthalene prevents the formation of products with the chlorinated periphery of the macrocycle. Substitution of chlorine atoms at titanium by oxygen with the formation of titanyl macrocycles was made by boiling of titanium dichloride macrocycles in wet pyridine (5% of H_2O).[33] Scheme 2 of the reactions is shown below.

The obtained titanyl macrocycles are reduced with sodium fluorenone ketyl in the presence of an excess of PPNCl. This leads to the dissolution of all titanyl macrocycles in the form of anions though, for example, neutral $O{=}Ti^{IV}(AceTPrzPz^{2-})$ is completely insoluble in *o*-dichlorobenzene. The reduction of $Ti^{IV}Cl_2(Nc^{2-})$ with sodium fluorenone ketyl is accompanied by the substitution of chloride anions by oxygen at titanium(IV) atoms. Oxygen originates from fluorenone ketyl, and salt **2** with the $\{O{=}Ti^{IV}(Nc^{\bullet 3-})\}^{\bullet -}$ radical anions is formed.

According to redox potentials,[34–36] the naphthalocyanine macrocycle shows weaker acceptor properties than tetrapyrazinoporphyrazine and phthalocyanine macrocycles with electron-withdrawing chloro- and pyrazino-substituents. As a result, the reduction of $Ti^{IV}Cl_2Nc$ produces radical anion salt **2**, whereas the reduction of $O{=}Ti^{IV}(PcCl_8)$ and $O{=}Ti^{IV}(AceTPrzPz)$ under the same reaction conditions leads to the formation of dianion salts **1** and **3**.

Spectra of salts in the IR and UV-visible-NIR ranges

According to the composition titanyl naphthalocyanine should have −1 charge owing to the titanyl macrocycle : cation ratio of 1 : 1 in salt **2**, whereas the titanyl macrocycle : cation ratio of 1 : 2 in salts **1** and **3** shows the formation of titanyl macrocycle dianions (2−).

The IR spectra of the parent compounds and their salts are shown in Fig. S1–S3† and the observed absorption bands are listed in Table S1.† Titanyl macrocycles show absorption bands attributed to the Ti=O stretching mode. The absorption band of this mode is manifested at 946 cm^{-1} in the spectra of $O{=}Ti^{IV}(PcCl_8^{2-})$ and salt **1**. The Ti=O stretching mode is split into three bands manifested at 927, 947 and 974 cm^{-1} in the spectrum of $O{=}Ti^{IV}(AceTPrzPz^{2-})$. These bands are shifted to lower wavenumbers at 917, 927 and 941 cm^{-1} in the spectrum of **3** indicating the elongation of the Ti=O bonds in this salt. Salt **2** was obtained in the reduction of $Ti^{IV}Cl_2(Nc^{2-})$ with sodium fluorenone ketyl with the formation of $\{O{=}Ti^{IV}(Nc^{\bullet 3-})\}^{\bullet -}$ and the appearance of a new Ti=O bond. That is accompanied by the manifestation of a new band at 974 cm^{-1}. Earlier it was shown that the reduction of unsubstituted $O{=}Ti^{IV}(Pc^{2-})$ in $(Bu_4N^+)\{O{=}Ti^{IV}(Pc^{\bullet 3-})\}^{\bullet -}$ and

$(Et_4N^+)\{O{=}Ti^{IV}(Pc^{\bullet 3-})\}^{\bullet -}{\cdot}C_6H_4Cl_2$ is accompanied by the elongation of Ti=O bonds since the corresponding absorption bands are shifted from 962 to 923–928 cm^{-1}.[13]

The spectra of the starting titanyl macrocycles and salts **1–3** in KBr pellets in the UV-visible-NIR range are shown in Fig. 1. Unsubstituted $O{=}Ti^{IV}(Pc^{2-})$ shows the Soret band at 347 nm and the split Q-band at 654 and 708 nm.[20] The Soret and Q-bands have a close position in the spectra of $O{=}Ti^{IV}(PcCl_8{}^{2-})$ and $O{=}Ti^{IV}(AceTPrzPz^{2-})$ manifesting at 353, 660, 706 nm and 331, 652, 710 nm, respectively. Unsubstituted $Ti^{IV}Cl_2(Pc^{2-})$ shows absorption bands at 352, 665 and 721 nm. Linear annulation in the naphthalocyanine macrocycle of $Ti^{IV}Cl_2(Nc^{2-})$ results in a blue shift of the Soret band up to 340 nm and a strong red shift of the Q-band up to 753 and 834 nm (Fig. 1).

The spectra of **1–3** (Table 1) allow one to study how the reduction affects the optical properties of titanyl macrocycles. Analysis of these spectra shows that Soret bands are blue shifted in the reduction of the macrocycle in **1** and **3** whereas maxima of the Q-bands are strongly blue shifted in the spectra of **1** and **2**, but remain nearly unshifted in the spectrum of **3** (Table 1 and Fig. 1). The most pronounced changes in the formation of radical anions and dianions of titanyl macrocycles are the appearance of new intense NIR bands. The presence of these bands unambiguously allows one to determine the formation of reduced macrocycle anions. The blue shift of the Soret and Q bands and the appearance of NIR bands are characteristic of the radical anion salts of $\{O{=}Ti^{IV}(Pc^{\bullet 3-})\}^{\bullet -}$ and other metal phthalocyanines.[20,21] It should be noted that the NIR band in the spectrum of **2** (1159 nm) is strongly red shifted in comparison with the spectra of the $[O{=}Ti^{IV}(Pc^{\bullet 3-})]^{\bullet -}$ salts (995–998 nm).[20] At the same time these bands are observed almost at the same position in the spectra of **1** and **3** (999 and 963 nm, respectively). Thus, linear annulation in naphthalocyanine essentially strongly decreases the energy of the Q band and the NIR band of the radical anion even in comparison with those for tetra(acenaphthenopyrazino)porphyrazine which has essentially a larger π-system but no linear annulation. The spectra of **1** and **2** also show broad low-energy bands at 1550 and 1672 nm (Fig. 1), respectively, which can be attributed to the charge transfer between macrocycles as will be discussed in the next section. This band is not observed in the spectrum of **3** (Fig. 1), probably due to the ineffective overlapping between the $\{O{=}Ti^{IV}(AceTPrzPz^{4-})\}^{2-}$ dianions.

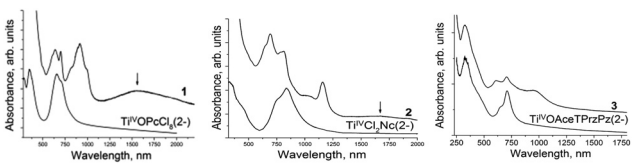

Fig. 1 UV-visible-NIR spectra of the starting titanyl macrocycles and salts **1–3** in KBr pellets prepared under anaerobic conditions. Charge transfer bands (CTB) are shown by arrows.

Molecular and crystal structures of salts 1–3

Geometric parameters of macrocycles in **1–3** are presented in Table 2. The average lengths of the Ti–N(Pc) bonds in **1–3** are 2.068(2)–2.097(6) Å. That is slightly longer than those in $\{O{=}Ti^{IV}(Pc^{\bullet 3-})\}^{\bullet -}$ (2.055(1)–2.062(1) Å).[20] The elongation of the Ti–N(Pc) bonds results in a stronger displacement of the Ti atoms from the 24-atom Pc plane which is maximal for the $\{O{=}Ti^{IV}(AceTPrzPz^{4-})\}^{2-}$ dianions in **3**. The length of the O=Ti bond also varies from 1.615(6) to 1.645(5) Å, and the shortest bonds are observed for the macrocycles with an extended π-system in **2** and **3**.

The reduction of the Pc macrocycle is accompanied by a transition from an aromatic 18 electron π-system to antiaromatic 19 and 20 electron π-systems for radical trianion and tetraanion macrocycles, respectively. As a result, partial disruption of the aromaticity of the macrocycles is observed in the reduced state leading to the alternation of the $C{-}N_{imine}$ bonds.[7–11,20,21] Such alternation is also observed for the reduced macrocycles in **1–3** (Table 2), but the difference between the shorter and longer $C{-}N_{imine}$ bonds in **1** and **3** with tetraanion macroheterocycles is nearly two times larger

Table 1 Data of UV-visible-NIR spectra of the starting titanyl macrocycles and salts **1–3**

	Position of the absorption band of phthalocyanines, nm		
Compound	Soret band, nm	Q-band, nm	Bands in NIR, nm
$O{=}Ti^{IV}(Pc^{2-})$[20]	347	654, 708	—
$(TBA^+)\{O{=}Ti^{IV}(Pc^{\bullet 3-})\}^{\bullet -}$ (ref. 20)	343	597, 630, 701	844 (weak), 995
$(TEA^+)\{O{=}Ti^{IV}(Pc^{\bullet 3-})\}^{\bullet -}{\cdot}C_6H_4Cl_2$ [20]	340	600, 630, 698	911 (weak), 998 1475 (CT band)
$O{=}Ti^{IV}(PcCl_8{}^{2-})$	353	660 (max), 706	—
$(PPN^+)_2\{O{=}Ti^{IV}(PcCl_8{}^{4-})\}^{2-}$ (**1**)	340	637 (max), 703	818, 916, 999 1550 (CT band)
$Ti^{IV}Cl_2(Pc^{2-})$	352	665(sh), 721 (max)	—
$Ti^{IV}Cl_2(Nc^{2-})$	340	753, 834 (max)	—
$(PPN^+)\{O{=}Ti^{IV}(Nc^{\bullet 3-})\}^{\bullet -}{\cdot}$(solvent) (**2**)	340	697 (max), 814	1040 (weak), 1159, 1672 (CT band)
$O{=}Ti^{IV}(AceTPrzPz^{2-})$	331	652 (weak), 710 (max)	—
$(PPN^+)_2\{O{=}Ti^{IV}(AceTPrzPz^{4-})\}^{2-}$ (solvent) (**3**)	325	607, 706 (max)	963

sh – shoulder; max – maximum.

Table 2 Geometric parameters of titanyl macrocycles in the neutral, radical anion and dianion state

Compound	Average length of bonds and contacts, Å			Displacement of atoms from the 24-atom Pc plane, Å	
	M–$N_{pyrrole}$	C–$N_{pyrrole}$	C–$N_{imine\ short/long,\ difference}$	Metal	$N_{pyrrole}$
O=$Ti^{IV}(Pc^{2-})$ ($P2_1/c$) O=Ti (1.628(3) Å)[24]	2.067(6)	1.374(6)	1.330(6)	0.778	0.091–0.184
O=$Ti^{IV}(Pc^{2-})$ (Cc) O=Ti (1.643(3) Å)[25] (both made by Rietveld analysis)	2.071(5)	1.375(5)	1.329(5)	0.742	0.076–0.151
$(Bu_4N^+)\{O{=}Ti^{IV}(Pc^{\bullet 3-})\}^{\bullet -}$ O=Ti (1.640(1) Å)[20]	2.062(1)	1.386(2)	1.325(2)/1.350(2), 0.025	0.711	0.084–0.135
$(Et_4N^+)\{O{=}Ti^{IV}(Pc^{\bullet 3-})\}^{\bullet -}{\cdot}C_6H_4Cl_2$ (O=Ti (1.657(1) Å))[20]	2.055(1)	1.388(2)	1.312(2)/1.351(2), 0.039	0.595	0.004–0.031
$(PPN^+)_2\{O{=}Ti^{IV}(PcCl_8{}^{4-})\}^{2-}$ (**1**) O=Ti (1.645(5) Å)	2.072(3)	1.390(4)	1.304(4)/1.375(4), 0.071	0.602	0.015–0.019
$(PPN^+)\{O{=}Ti^{IV}(Nc^{\bullet 3-})\}^{\bullet -}$(solvent) (**2**) O=Ti (1.638(2) Å)	2.068(2)	1.397(3)	1.315(3)/1.353(3), 0.038	0.556	0.007–0.088
$(PPN^+)_2\{O{=}Ti^{IV}(AceTPrzPz^{4-})\}^{2-}$ (solvent) (**3**) (O=Ti (1.615(6) Å))	2.097(6)	1.402(9)	1.314(9)/1.374(9), 0.060	0.741	0.067–0.166

than those for the radical trianion $Pc^{\bullet 3-}$ (ref. 20) and $Nc^{\bullet 3-}$ macrocycles (Table 2). Thus, disruption of aromaticity is more pronounced for the dianion titanyl macrocycles. Alternation of bonds is realized in such a way that shorter and longer C–N_{imine} bonds belong to two oppositely located isoindole units in **1–3** as is also observed in the radical anions of other metal phthalocyanines.[20,21]

A half of $\{O{=}Ti^{IV}(PcCl_8{}^{4-})\}^{2-}$ dianion and one PPN^+ cation are independent in **1**. These dianions form layers in the *ab* plane (Fig. 2a), which are separated by the PPN^+ cations (Fig. 2b). More closely packed chains can be outlined along the *a* axis within the phthalocyanine layers (Fig. 2a). Each phthalocyanine macrocycle has four short van der Waals (vdW) C···C and Cl···Cl contacts of about 3.5 Å length with the neighboring dianions in these chains. The interplanar distance in the chains is uniform and is rather short (3.38 Å). Most probably namely close packing of the $PcCl_8$ macrocycles in **1** provides the appearance of an intense charge transfer band in the NIR spectrum (see above). Any vdW contacts between phthalocyanines from the neighboring chains within the layer are absent. The macrocycle is almost flat in **1** with only slight deviations of atoms from the 24-atom Pc plane (less than 0.065 Å).

One $\{O{=}Ti^{IV}(Nc^{\bullet 3-})\}^{\bullet -}$ radical anion, one PPN^+ cation and two solvent $C_6H_4Cl_2$ molecules are independent in **2**. There are naphthalocyanine chains along the *a* axis (Fig. 3) which are

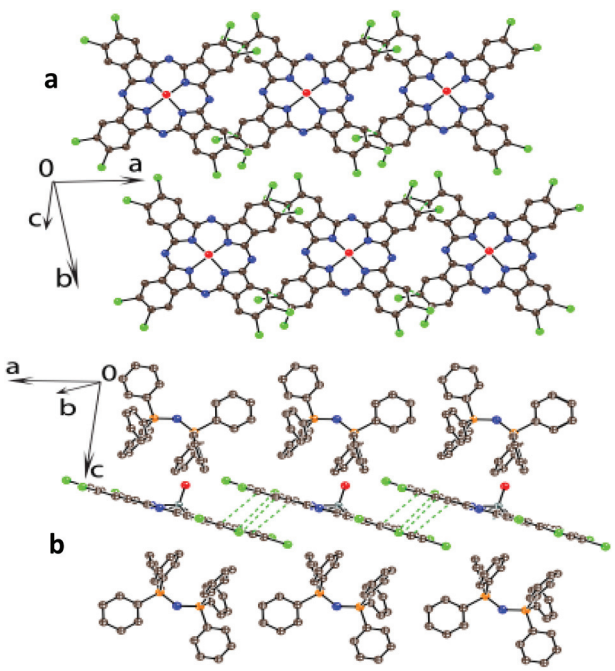

Fig. 2 Crystal structure of $(PPN^+)_2\{O{=}Ti^{IV}(PcCl_8{}^{4-})\}^{2-}$ (**1**). Views perpendicular (a) and parallel (b) to the phthalocyanine layers. Shortened vdW C,Cl···C,Cl contacts are shown by green dashed lines.

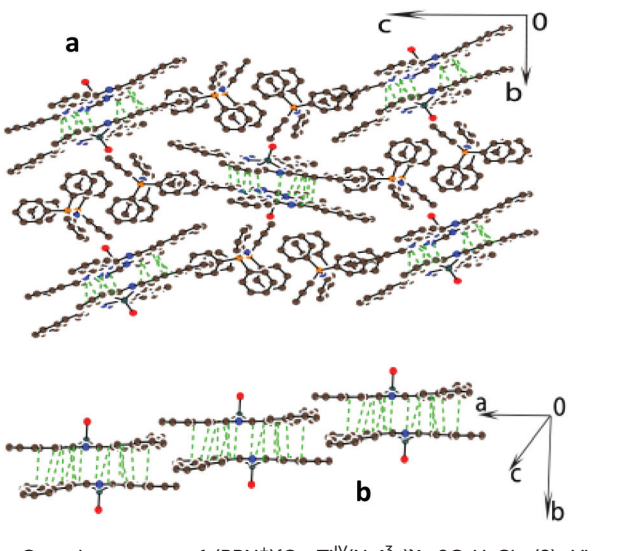

Fig. 3 Crystal structure of $(PPN^+)\{O{=}Ti^{IV}(Nc^{\bullet 3-})\}^{\bullet -}{\cdot}2C_6H_4Cl_2$ (**2**). View along the *a* axis and the naphthalocyanine chains (a) and view on these chains (b). Shortened vdW C,N···C,N contacts are shown by green dashed lines. Solvent molecules are not shown for clarity.

isolated by the PPN^+ cations. The $\{O{=}Ti^{IV}(Nc^{\bullet 3-})\}^{\bullet -}$ radical anions form dimers in these chains with multiple C,N···C,N vdW contacts, but macrocycles in these dimers are only slightly shifted relative to each other. As a result, there are no short vdW contacts between the neighboring dimers within the chains. The naphthalocyanine macrocycle has two adjacent naphthalene groups located strictly above the 24-atom plane, whereas two other groups are located almost in the plane. The interplanar distance of 3.169 Å is very short in the dimer indicating effective π–π interaction between the macrocycles in **2** explaining the appearance of a charge transfer (CT) band in the NIR spectrum. The interplanar distance in **2** is close to that in previously studied $(Et_4N^+)\{O{=}Ti^{IV}(Pc^{\bullet 3-})\}^{\bullet -}{\cdot}C_6H_4Cl_2$ salt (3.129 Å) which also shows an intense CT band in the NIR range.[20]

As a result of strong disorder of solvent molecules, the structure of **3** was refined with a relatively high *R*-factor value (0.1158).

Nevertheless, the structures of the $\{O{=}Ti^{IV}(AceTPrzPz^{4-})\}^{2-}$ dianion and the PPN^+ cations were determined quite reliably. Dianions form the $[\{O{=}Ti^{IV}(AceTPrzPz^{4-})\}^{2-}]_2$ dimers with a strong shift of the macrocycles but effective π–π stacking between one of four acenaphthenopyrazino groups of the $\{O{=}Ti^{IV}(AceTPrzPz^{4-})\}^{2-}$ dianions (Fig. 4a and b).

The interplanar distance between them is 3.38 Å and the shortest C,N···C,N vdW contacts are in the 3.19–3.36 Å range. The dihedral angle between the planes of the acenaphthenopyrazino groups of neighboring dianions in the dimer is only 0.22° showing their parallel arrangement. The strong shift of the macroheterocycles relative to each other in the dimers leads to the formation of chains arranged along the [1–1–0] direction (Fig. 4c and d). There are 4 C···C vdW contacts between the neighboring dimers in these chains of 3.47–3.56 Å length. These contacts are of π-type since the acenaphthene planes of two dianions involved in this interaction are nearly parallel (the dihedral angle between them is 8.12°) and the interplanar distance is only 3.42 Å. There are also several side-by-side vdW C···C contacts of 3.31 Å length between the $[\{O{=}Ti^{IV}(AceTPrzPz^{4-})\}^{2-}]_2$ dimers from the neighboring chains (Fig. 4c, green dashed lines). The macrocycle in **3** has concave conformation and deviates strongly from planarity in contrast to the geometry of the macrocycles in **1** and **2**.

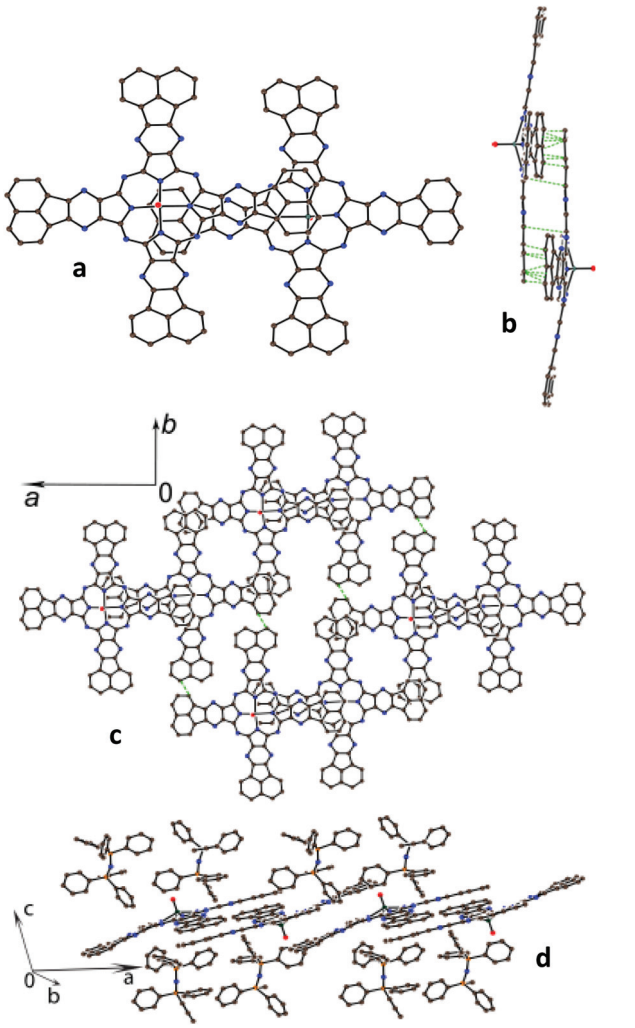

Fig. 4 Crystal structure of $(PPN^+)_2\{O{=}Ti^{IV}(AceTPrzPz^{4-})\}^{2-}{\cdot}1.2C_6H_4Cl_2{\cdot}0.8C_6H_4Cl_2$ (**3**): view on (a) and along (b) the $[\{O{=}Ti^{IV}(AceTPrzPz^{4-})\}^{2-}]_2$ dimer, view on (c) and along (d) the layers from the dimers. Shortened vdW C···C contacts are shown by green dashed lines. Solvent molecules are not shown for clarity.

EPR studies of the salts

The EPR spectra of salts **1** and **3** at 300 K contain weak asymmetric signals which can be approximated by three lines with g = 1.9975–2.0042 and the linewidth (ΔH) = 0.45–0.92 mT, which are characteristic of the radical anions of phthalocyanine species. The intensity of these signals is very low (less than 1% of spins from the total amount of titanyl macrocycle). Therefore, the signals can be most probably attributed to paramagnetic impurities. Thus, the $\{O{=}Ti^{IV}(PcCl_8^{4-})\}^{2-}$ and $\{O{=}Ti^{IV}(AceTPrzPz^{4-})\}^{2-}$ dianions are diamagnetic.

Salt **2** shows an asymmetric EPR signal which can be simulated well by two narrow lines (g_1 = 2.0034 and ΔH = 0.50 mT, g_2 = 2.0014 and ΔH = 0.88 mT) and one broad line with g_3 = 2.0018 and ΔH = 4.67 mT at 300 K (Fig. 5).

Narrow lines can be attributed to paramagnetic impurities due to that their intensities are less than 3% from that of the broad signal. The broad line decreases seven times in intensity upon cooling the sample from 300 down to 200 K (Fig. 5b). Below 200 K all three lines are of low intensity and show paramagnetic temperature dependence down to 4 K. Thus, salt **2** is diamagnetic below 200 K. The crystal structure of **2** shows that the $\{O{=}Ti^{IV}(Nc^{\bullet 3-})\}^{\bullet -}$ radical anions form closely packed π-stacking $[\{O{=}Ti^{IV}(Nc^{\bullet 3-})\}^{\bullet -}]_2$ dimers that can provide strong coupling between them. As a result, a diamagnetic singlet state with an antiparallel arrangement of spins in the dimers is formed below 200 K. A triplet state of the dimers with a parallel arrangement of spins is populated above 200 K. The observed singlet–triplet transition in **2** is similar to that

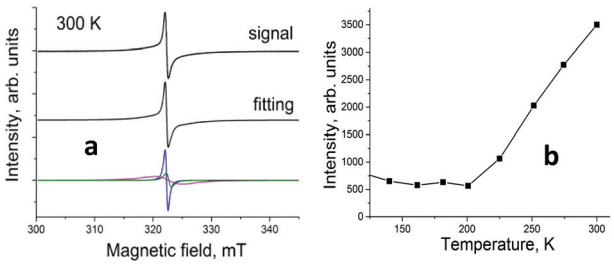

Fig. 5 EPR spectrum of **2** at 300 K (a). Temperature dependence of the main component of EPR signal of salt **2** (b).

observed in $(Et_4N^+)\{O{=}Ti^{IV}(Pc^{\bullet 3-})\}^{\bullet -}{\cdot}C_6H_4Cl_2$ which also contains π-stacking $[\{O{=}Ti^{IV}(Pc^{\bullet 3-})\}^{\bullet -}]_2$ dimers. However, the temperature of the transition to the singlet state in **2** (200 K) is higher than that in $(Et_4N^+)\{O{=}Ti^{IV}(Pc^{\bullet 3-})\}^{\bullet -}{\cdot}C_6H_4Cl_2$ (150 K).[20] This can be explained by stronger π–π interactions in **2**, probably due to the larger π-system of the naphthalocyanine macrocycle.

Conclusions

A series of radical anion and dianion salts based on titanyl macrocycles with acceptor substituents or an extended π-system were obtained as single crystals for the first time. The reduction of titanyl macrocycles in the presence of bulky PPN^+ cations allows their dissolution due to the formation of the radical anions or dianions, whereas they are very weakly soluble in organic solvents in the neutral state. Thus, titanyl macrocycles can be crystallized and their molecular structures are determined from X-ray diffraction on single crystals. Extension of a π-system by linear annulation in naphthalocyanine leads to a strong red shift of the Q-band and NIR bands of the radical anions, whereas tetra(acenaphthenopyrazino) porphyrazine with an extended π-system shows Q-bands and a NIR band of the anions nearly at the same position as in the spectra of the salts with unsubstituted titanyl phthalocyanine radical anions, $\{O{=}Ti^{IV}(Pc^{\bullet 3-})\}^{\bullet -}$. Partial disruption of aromaticity is observed in the reduction of the macrocycles. This effect is more pronounced for the dianions than for the radical anions. Increased size of the macrocycle leads to the formation of π-stacked structures. In the case of **2** this provides effective magnetic coupling between the spins within the $[\{O{=}Ti^{IV}(Nc^{\bullet 3-})\}^{\bullet -}]_2$ dimers and the transition of the dimers to the singlet ground state even below 200 K (at a temperature higher than that in the $[\{O{=}Ti^{IV}(Pc^{\bullet 3-})\}^{\bullet -}]_2$ dimers). Macrocycles in **1** and **3** are packed in the π-stacked chains. However, the diamagnetic nature of the dianions does not allow one to expect the realization of conductivity or magnetic interactions in these chains. We suppose that the radical anions of these titanyl macrocycles can provide more promising magnetic properties. Preparation of these salts is now in progress.

Experimental

Materials

4,5-Dichlorophthalonitrile (Aldrich, 99%), 2,3-dicyanonaphthalene (TCI, 99%), acenaphthenequinone (Acros, 95%), and diaminomaleonitrile (Acros, 98%) were used as received. $TiCl_4$ (Aldrich, 99%) and $TiCl_4{\cdot}2THF$ (Aldrich, 97%) were used as received. Bis(triphenylphosphoranylidene)ammonium chloride (PPNCl) was purchased from Aldrich (98%). 1-Chloronaphthalene (Aldrich, technical grade) was used as received. Sodium fluorenone ketyl was obtained as described.[37] Solvents were purified under an argon atmosphere. *o*-Dichlorobenzene ($C_6H_4Cl_2$) was distilled over CaH_2 under reduced pressure; hexane was distilled over Na/benzophenone, and benzonitrile (C_6H_5CN) was distilled over Na under reduced pressure. The solvents were degassed and stored in a glove box. The crystals of **1–3** were stored in the glove box. KBr pellets for IR- and UV-visible-NIR measurements were also prepared in the glove box. EPR measurements were performed on polycrystalline samples of **1–3** sealed in 2 mm quartz tubes under 10^{-5} Torr.

Synthesis of titanyl macrocycles

Titanyl macrocycles (Scheme 2) were synthesized as described in ref. 33.

Titanyl 2,3,9,10,16,17,23,24-octachlorophthalocyanine, $O{=}Ti^{IV}(PcCl_8^{2-})$. 4,5-Dichlorophthalonitrile (1 g, 5.076 mmol), 2-methylnaphthalene (180 mg, 1.269 mmol) and $TiCl_4$ (0.14 ml, 1.269 mmol) in 10 ml of 1-chloronaphthalene were heated up to 250 °C upon stirring for 5 hours under an argon atmosphere. Then the reaction mixture was cooled down to 50 °C, the precipitate was filtered under reduced pressure and washed with toluene and methanol. $Ti^{IV}Cl_2(PcCl_8^{2-})$ was converted to $O{=}Ti^{IV}(PcCl_8^{2-})$ by boiling in wet pyridine (5% of H_2O) for two hours. $O{=}Ti^{IV}(PcCl_8^{2-})$ was filtered, washed with water and dried at 100 °C in a vacuum for 2 hours to yield 800 mg of blue powder (68%). Anal. found: C 44.86, N 13.01, H 1.12, Cl 33.21%. Calcd for $C_{32}H_8N_8Cl_8OTi$: C 45.08, N 13.15, H 0.94, Cl 33.34%. IR (KBr), ν, cm^{-1}: 3087m, 2922m, 2849w, 2353w, 1603m, 1471m, 1413s, 1375m, 1320m, 1069s, 980w, 945m, 890m, 829m, 775m, 705m, 659m, 463w, 431w. UV-VIS, KBr pellet λ_{max}, nm: 353, 660, 706.

Titanium(IV) 2,3-naphthalocyanine dichloride, $Ti^{IV}Cl_2(Nc^{2-})$. 2,3-Dicyanonaphthalene (1 g, 5.612 mmol), 2-methylnaphthalene (200 mg, 1.403 mmol) and $TiCl_4{\cdot}2THF$ (468 mg, 1.403 mmol) in 10 ml of 1-chloronaphthalene were heated up to 250 °C upon stirring for 5 hours under an argon atmosphere. Then the reaction mixture was cooled down to 50 °C and the precipitate was filtered under reduced pressure and washed with toluene and methanol. $Ti^{IV}Cl_2Nc$ was dried at 100 °C in a vacuum for 2 hours to yield 850 mg of dark green powder (73%). Anal. found: C 69.01, N 13.30, H 3.06, Cl 8.44%. Calcd for $C_{48}H_{24}N_8Cl_2Ti$: C 69.26, N 13.47, H 2.89, Cl 8.54%. IR (KBr), ν, cm^{-1}: 1747w, 1639m, 1468w, 1358m, 1338m, 1318m, 1153w, 1125m, 1062s, 1011m, 1077s, 968m, 886m, 863m, 798w, 752s, 733w, 716m, 690w, 656w, 514w, 488w, 469m. UV-VIS, KBr pellet λ_{max}, nm: 340, 753, 834.

Acenaphtho[1,2-*b*]pyrazine-8,9-dicarbonitrile. A mixture of acenaphthenequinone (2 g, 11 mmol) and an equimolar quantity of diaminomaleonitrile (1.187 g, 11 mmol) in 30 ml acetic acid was heated at 100 °C upon stirring for 1 hour. The residue was filtered off, washed with water and acetone (3 ml) and dried at 100 °C in a vacuum for 2 hours to yield 2.15 g of dark orange powder (77%).

Titanyl tetra(acenaphthenopyrazino)porphyrazine, O═Ti^{IV} (AceTPrzPz^{2-}). Acenaphtho[1,2-*b*]pyrazine-8,9-dicarbonitrile (1 g, 3.933 mmol), 2-methylnaphthalene (140 mg, 0.983 mmol) and $TiCl_4$ (0.11 mL, 0.983 mmol) in 10 ml of 1-chloronaphthalene were heated up to 250 °C upon stirring for 5 hours under an argon atmosphere. Then the reaction mixture was cooled down to 50 °C, the precipitate was filtered under reduced pressure and washed with toluene and methanol. Ti^{IV}Cl$_2$(AceTPrzPz^{2-}) was converted to O═Ti^{IV}(AceTPrzPz^{2-}) by boiling in wet pyridine (5% of H_2O) for two hours. O═Ti^{IV}(AceTPrzPz^{2-}) was filtered, washed with water and dried at 100 °C in a vacuum for 2 hours to yield 800 mg of black powder (75%). Anal. found: C 70.88, N 20.59, H 2.49%. Calcd for $C_{64}H_{24}N_{16}OTi$: C 71.04, N 20.72, H 2.22%. IR (KBr), ν, cm^{-1}: 2921m, 2851m, 1615s, 1514m, 1458m, 1431s, 1369w, 1333s, 1262m, 1229s, 1179m, 1134s, 1099m, 1033s, 974w, 947m, 927m, 828m, 772s, 716m, 675m, 660m, 630m, 559w, 464s, 449m. UV-VIS, KBr pellet λ_{max}, nm: 331, 652, 710.

Syntheses of crystalline salts 1–3

Crystals of **1–3** were obtained by the diffusion technique. The reaction solutions of salts **1–3** were filtered in a 50 mL glass tube of 1.8 cm diameter with a ground glass plug, and 30 mL of hexane was layered over the solution. Slow mixing of two solvents for 1.5 months provided precipitation of crystals on the walls of the tube. The solvent was decanted from the crystals and they were washed with hexane.

Salts (PPN)$_2${O═Ti^{IV}PcCl$_8$} (**1**) and (PPN){O═Ti^{IV}Nc}·2$C_6H_4Cl_2$ (**2**) were obtained by reduction of 34.6 mg of Ti^{IV}OPcCl$_8$ (0.042 mmol) or 35.5 mg of Ti^{IV}Cl$_2$Nc (0.042 mmol) with sodium fluorenone ketyl (55 mg, 0.27 mmol) in the presence of PPNCl (75 mg, 0.131 mmol) in 16 ml of *o*-dichlorobenzene for two hours at 100 °C until complete dissolution of the starting compounds and the formation of dark green and deep-blue-green solutions, respectively. The final solutions were filtered into a tube for diffusion. Black blocks of **1** and dark violet elongated prisms of **2** were obtained in 25 and 45% yield, respectively.

Salt (PPN)$_2${O═Ti^{IV}AceTPrzPz}·1.3$C_6H_4Cl_2$·0.8C_6H_5CN (**3**) was obtained by the reduction of 36 mg of O═Ti^{IV}AceTPrzPz (0.033 mmol) with sodium fluorenone ketyl (55 mg, 0.27 mmol) in the presence of PPNCl (75 mg, 0.131 mmol) in 18 ml of *o*-dichlorobenzene/benzonitrile mixture (15 : 3) for two hours at 100 °C until complete dissolution of phthalocyanine and the formation of a dark green solution. The final solution was filtered into a tube for diffusion. Black prisms were obtained in 15% yield.

The composition of **1–3** (Table 3) was determined from X-ray diffraction on single crystals. The analysis of the obtained crystals under a microscope in a glove box as well as testing of several single crystals from each synthesis by X-ray diffraction showed that only one crystalline phase is formed.

Table 3 X-ray diffraction data for salts **1–3**

Compound	**1**	**2**	**3**
Emp. formula	$C_{104}H_{68}Cl_8N_{10}OP_4Ti$	$C_{96}H_{62}Cl_4N_9OP_2Ti$	$C_{149.4}H_{93.2}Cl_{2.6}N_{18.8}OP_4Ti$
M_r [g mol^{-1}]	1929.06	1609.18	2431.57
Color and shape	Black, block	Dark-violet, prism	Black, prism
Crystal system	Triclinic	Monoclinic	Monoclinic
Space group	$P\bar{1}$	$P2_1/c$	$C2/c$
a, Å	11.3971(7)	15.1213(3)	36.695(2)
b, Å	14.8799(8)	18.0169(3)	25.1999(8)
c, Å	15.0231(9)	29.1976(6)	27.4198(11)
α, °	63.130(6)	90	90
β, °	77.450(8)	98.402(2)	101.073(5)
γ, °	78.459(8)	90	90
V, Å^3	2203.1(3)	7869.2(3)	24 883.5(19)
Z	1	4	8
ρ_{calc} [g cm^{-3}]	1.454	1.358	1.298
μ [mm^{-1}]	0.888	0.343	0.239
F(000)	988	3316	10 043
T [K]	100(2)	150(2)	100(2)
Max. 2Θ, °	73.500	58.748	50.000
Reflns measured	32 780	100 772	68 100
Unique reflns	8464	20 327	20 895
Parameters	586	1035	1529
Restraints	0	1238	797
Reflns [$F_o > 2(F_o)$]	7252	15 449	11 354
R_1 [$F_o > 2\sigma(F_o)$]	0.0613	0.0818	0.1158
wR_2 (all data)	0.1468	0.1824	0.3277
G.O.F	0.998	1.105	1.063
CCDC number	1518488	1518412	1518411

Elemental analysis cannot be used to determine the composition of the obtained crystals due to their high air sensitivity and an addition of oxygen during the procedure of elemental analysis.

General

UV-visible-NIR spectra were obtained using KBr pellets on a PerkinElmer Lambda 1050 spectrometer in the 250–2500 nm range. FT-IR spectra were obtained using KBr pellets with a PerkinElmer Spectrum 400 spectrometer (400–7800 cm^{-1}). EPR spectra were recorded on polycrystalline samples of **1–3** from 4 up to 295 K and back from 295 to 150 K for **2** with a JEOL JES-TE 200 X-band ESR spectrometer equipped with a JEOL ES-CT470 cryostat.

Crystal structure determination

Crystallographic data for **1–3** are listed in Table 3. Synchrotron X-ray data for **1** were collected at 100 K on the BL14.3 at the BESSY storage ring (Berlin, Germany) using a MAR225 detector, $\lambda = 0.8950$ Å.

The data for **2** and **3** were collected on an Oxford diffraction "Gemini-R" CCD diffractometer with graphite monochromated MoK_α radiation at low temperature using an Oxford Instrument Cryojet cooler. Experimental data were processed using CrysAlisPro software, Oxford Diffraction Ltd, raw data reduction to F^2 was carried out using Bruker SAINT.[38] The structures were solved by direct methods and refined by the full-matrix least-squares method against F^2 using SHELX-2013 and 2014.[39] Non-hydrogen atoms were refined in the anisotropic approximation. Positions of hydrogen atoms were calculated geometrically.

The Ti1 and O1 atoms in structure **1** are disordered around an inversion center. The structure of **2** contains one strongly disordered $C_6H_4Cl_2$ molecule with the 0.355(3)/0.275(3)/0.231(3)/0.139(3) occupancies. In the structure of **3** there are completely ordered $\{O{=}Ti^{IV}(AceTPrzPz^{4-})\}^{2-}$ dianion and one and two halves of independent PPN^+ cations. One and half independent PPN^+ cations contain one statistically disordered phenyl group. Two positions of solvent molecules contain strongly disordered $C_6H_4Cl_2$ and C_6H_5CN molecules. Due to the strong disorder of some solvent molecules in **2** and **3** and phenyl substituents of PPN^+ in **3**, multiple restraints were used for the crystal structure refinement of these salts. To keep the solvent and phenyl geometry close to the ideal one in the disordered groups, the bond length restraints were applied along with the next-neighbor distances using the SADI SHELXL instruction. To keep the anisotropic thermal parameters of the disordered groups within reasonable limits the displacement components were restrained using the SIMU and DELU SHELXL instructions.

Acknowledgements

The reported study was funded by RFBR according to the research project no. 16-33-00588 mol_a.

Notes and references

1 C. G. Claessens, W. J. Blau, M. Cook, M. Hanack, R. J. M. Nolte, T. Torres and D. Wöhrle, *Monatsh. Chem.*, 2001, **132**, 3.
2 D. Wöhrle, G. Schnurpfeil, S. G. Makarov, A. Kazarin and O. N. Suvorova, *Macroheterocycles*, 2012, **5**, 191.
3 D. C. Y. Ethelbhert, M. Matsuda, H. Tajima, A. Kikuchi, T. Taketsugu, N. Hanasaki, T. Naito and T. Inabe, *J. Mater. Chem.*, 2009, **19**, 718.
4 T. Inabe and H. Tajima, *Chem. Rev.*, 2004, **104**, 5503.
5 D. K. Rittenberg, L. Baars-Hibbe, A. B. Böhm and J. S. Miller, *J. Mater. Chem.*, 2000, **10**, 241.
6 D. V. Konarev, L. V. Zorina, S. S. Khasanov, E. U. Hakimova and R. N. Lyubovskaya, *New J. Chem.*, 2012, **36**, 48.
7 E. W. Y. Wong and D. B. Leznoff, *J. Porphyrins Phthalocyanines*, 2012, **16**, 154.
8 J. A. Cissell, T. P. Vaid, A. G. DiPasquale and A. L. Rheingold, *Inorg. Chem.*, 2007, **46**, 7713.
9 J. A. Cissell, T. P. Vaid and A. L. Rheingold, *Inorg. Chem.*, 2006, **45**, 2367.
10 E. W. Y. Wong, C. J. Walsby, T. Storr and D. B. Leznoff, *Inorg. Chem.*, 2010, **49**, 3343.
11 W. Zhou, R. H. Platel, T. T. Tasso, T. Furuyama, N. Kobayashi and D. B. Leznoff, *Dalton Trans.*, 2015, **44**, 13955.
12 M. Tahiri, P. Doppelt, J. Fischer and R. Weiss, *Inorg. Chim. Acta*, 1987, **127**, L1.
13 D. V. Konarev, A. V. Kuzmin, S. V. Simonov, S. S. Khasanov, A. Otsuka, H. Yamochi, G. Saito and R. N. Lyubovskaya, *Dalton Trans.*, 2012, **41**, 13841.
14 H. Hückstädt and H. Homborg, *Z. Anorg. Allg. Chem.*, 1998, **624**, 715.
15 D. V. Konarev, S. S. Khasanov, M. Ishikawa, A. Otsuka, H. Yamochi, G. Saito and R. N. Lyubovskaya, *Inorg. Chem.*, 2013, **52**, 3851.
16 D. V. Konarev, A. V. Kuzmin, S. S. Khasanov and R. N. Lyubovskaya, *Dalton Trans.*, 2013, **42**, 9870.
17 D. V. Konarev, L. V. Zorina, M. Ishikawa, S. S. Khasanov, A. Otsuka, H. Yamochi, G. Saito and R. N. Lyubovskaya, *Cryst. Growth Des.*, 2013, **13**, 4930.
18 D. V. Konarev, A. V. Kuzmin, M. Ishikawa, Y. Nakano, M. A. Faraonov, S. S. Khasanov, A. Otsuka, H. Yamochi, G. Saito and R. N. Lyubovskaya, *Eur. J. Inorg. Chem.*, 2014, 3863.
19 D. V. Konarev, L. V. Zorina, S. S. Khasanov, A. L. Litvinov, A. Otsuka, H. Yamochi, G. Saito and R. N. Lyubovskaya, *Dalton Trans.*, 2013, **42**, 6810.
20 D. V. Konarev, A. V. Kuzmin, M. A. Faraonov, M. Ishikawa, S. S. Khasanov, A. Otsuka, H. Yamochi, G. Saito and R. N. Lyubovskaya, *Chem. – Eur. J.*, 2015, **21**, 1014.
21 D. V. Konarev, S. I. Troyanov, M. Ishikawa, M. A. Faraonov, A. Otsuka, H. Yamochi, G. Saito and R. N. Lyubovskaya, *J. Porphyrins Phthalocyanines*, 2014, **18**, 1157.
22 D. V. Konarev, A. V. Kuzmin, S. S. Khasanov, A. Otsuka, H. Yamochi, G. Saito and R. N. Lyubovskaya, *Dalton Trans.*, 2014, **43**, 13061.

23 M. Tanaka, in *High Performance Pigments*, ed. E. B. Faulkner and R. J. Schwartz, Wiley-VCH, Weinheim, 2009, p. 275.
24 K.-Y. Law, *Chem. Rev.*, 1993, **93**, 449.
25 Y. Wang and D. Liang, *Adv. Mater.*, 2010, **22**, 1521.
26 H.-J. Kang, E.-H. Kang, S.-W. Park, J.-W. Lee and J.-K. Lee, *Macromol. Symp.*, 2006, **235**, 195.
27 M. Mayukh, C. M. Sema, J. M. Roberts and D. V. McGrath, *J. Org. Chem.*, 2010, **21**, 7893.
28 (*a*) E. A. Lukyanets and V. N. Nemykin, *J. Porphyrins Phthalocyanines*, 2010, **14**, 1; (*b*) V. N. Nemykin and E. A. Lukyanets, *ARKIVOC*, 2010, (Part 1), 136; (*c*) E. A. Lukyanets and V. N. Nemykin, in *Handbook of porphyrin science with applications to chemistry, physics, materials science, engineering, biology and medicine: synthetic methodology*, Series Handbook of Porphyrin Science, 2010, vol. 3, pp. 1–323.
29 K. Oka, O. Okada and K. Nukada, *Jpn. J. Appl. Phys.*, 1992, **31**, 2181.
30 O. Okada, K. Oka and M. Iijima, *Jpn. J. Appl. Phys.*, 1993, **32**, 3556.
31 A. J. Ramadan, L. A. Rochford, D. S. Keeble, P. Sullivan, M. P. Ryan, T. S. Jones and S. Heutz, *J. Mater. Chem. C*, 2015, **3**, 461.
32 M. P. Donzello, C. Ercolani, V. Novakova, P. Zimcik and P. A. Stuzhin, *Coord. Chem. Rev.*, 2016, **309**, 107.
33 L. A. Tomachynsk, V. Ya. Chernii and S. V. Volkov, *Russ. J. Inorg. Chem.*, 2002, **47**, 208.
34 A. B. P. Lever, E. R. Milaeva and G. Speier, in *Phthalocyanines: Properties and Applications*, ed. C. C. Leznoff and A. B. P. Lever, VCH Publishers, Inc., New York, 1993, vol. 3, p. 1.
35 K. Takahashi, Y. Aoki, T. Sugitani, F. Moriyama, Y. Tomita, M. Handa, K. Kasuga and K. Sogabe, *Inorg. Chim. Acta*, 1992, **201**, 247.
36 B. L. Wheeler, G. Nagasubramanian, A. J. Bard, L. A. Schechtman, D. R. Dininny and M. E. Kenney, *J. Am. Chem. Soc.*, 1984, **106**, 7405.
37 D. V. Konarev, S. S. Khasanov, E. I. Yudanova and R. N. Lyubovskaya, *Eur. J. Inorg. Chem.*, 2011, 816.
38 Bruker AXS Inc., Madison, Wisconsin, USA.
39 G. M. Sheldrick, *Acta Crystallogr., Sect. A: Fundam. Crystallogr.*, 2008, **64**, 112.